



RNase A Promotes Proliferation of Neuronal Progenitor Cells via an ERK-Dependent Pathway

Hsin-Yu Liu^{†‡}, Chiung-Ya Chen[†], Yun-Fen Hung, Hong-Ru Lin, Hsu-Wen Chao[‡], Pu-Yun Shih, Chi-Ning Chuang, Wei-Ping Li, Tzyy-Nan Huang and Yi-Ping Hsueh^{*}

Institute of Molecular Biology, Academia Sinica, Taipei, Taiwan

OPEN ACCESS

Edited by:

Enrico Tongiorgi,
University of Trieste, Italy

Reviewed by:

Daniele Bottai,
Università Degli Studi di Milano, Italy
Tara Louise Walker,
University of Queensland, Australia

*Correspondence:

Yi-Ping Hsueh
yph@gate.sinica.edu.tw

[†]These authors have contributed
equally to the work

‡Present Address:

Hsin-Yu Liu,
La Jolla Institute for Allergy and
Immunology, La Jolla, CA,
United States
Hsu-Wen Chao,
Department of Physiology, School of
Medicine, College of Medicine, Taipei
Medical University, Taipei, Taiwan

Received: 27 August 2018

Accepted: 05 November 2018

Published: 26 November 2018

Citation:

Liu H-Y, Chen C-Y, Hung Y-F, Lin H-R,
Chao H-W, Shih P-Y, Chuang C-N,
Li W-P, Huang T-N and Hsueh Y-P
(2018) RNase A Promotes
Proliferation of Neuronal Progenitor
Cells via an ERK-Dependent Pathway.
Front. Mol. Neurosci. 11:428.
doi: 10.3389/fnmol.2018.00428

Members of the ribonuclease A (RNase A) superfamily regulate various physiological processes. RNase A, the best-studied member of the RNase A superfamily, is widely expressed in different tissues, including brains. We unexpectedly found that RNase A can trigger proliferation of neuronal progenitor cells (NPC) both *in vitro* and *in vivo*. RNase A treatment induced cell proliferation in dissociated neuronal cultures and increased cell mass in neurosphere cultures. BrdU (5-Bromo-2'-Deoxyuridine) labeling confirmed the effect of RNase A on cell proliferation. Those dividing cells were Nestin- and SOX2-positive, suggesting that RNase A triggers NPC proliferation. The proliferation inhibitor Ara-C completely suppressed the effect of RNase A on NPC counts, further supporting that RNase A increases NPC number mainly by promoting proliferation. Moreover, we found that RNase A treatment increased ERK phosphorylation and blockade of the ERK pathway inhibited the effect of RNase A on NPC proliferation. Intracerebroventricular injection of RNase A into mouse brain increased the population of 5-ethynyl-2'-deoxyuridine (EdU) or BrdU-labeled cells in the subventricular zone. Those RNase A-induced NPCs were able to migrate into other brain areas, including hippocampus, amygdala, cortex, striatum, and thalamus. In conclusion, our study shows that RNase A promotes proliferation of NPCs via an ERK-dependent pathway and further diversifies the physiological functions of the RNase A family.

Keywords: ERK activation, neural progenitor cells, neurogenesis, proliferation, RNase A

INTRODUCTION

The ribonuclease A (RNase A) superfamily consists of thirteen members in human (Cho et al., 2005; Gupta et al., 2013). Bovine RNase A, the best-characterized member of the RNase A family, was originally isolated from bovine pancreas. Human RNase 1, the RNase A ortholog, shares ~70% amino acid sequence identity with bovine RNase A (Beintema, 1998; Koczera et al., 2016). Hereafter in this report, RNase A describes either RNase A or RNase 1. The RNase A superfamily consists of secreted proteins that are expressed in a wide range of tissues, including brain (Gupta et al., 2013). They share similar primary sequences and a common disulfide-bonded tertiary conformation (Beintema, 1998). Though sequences are similar, the mammalian RNase A superfamily is one of the most rapidly-evolving gene families in mammals (Cho et al., 2005), which may be relevant to the versatile functions of this family, including anti-bacterial and anti-viral activities (Rosenberg, 2008; Gupta et al., 2013; Rademacher et al., 2016), inhibition or promotion of tumor growth and

metastasis (Suzuki et al., 1999; Mironova et al., 2013, 2017; Chen et al., 2015; Attery et al., 2018; Wang et al., 2018), angiogenesis (Folkman and Klagsbrun, 1987; Gao and Xu, 2008; Sheng and Xu, 2016; Lyons et al., 2017), and cell proliferation (Li et al., 2013; Yu et al., 2017; Wang et al., 2018).

As a secreted protein, RNase A and other superfamily members are involved in the degradation of extracellular single-stranded RNA (ssRNA), though their enzymatic activities vary (Lyons et al., 2017). The extracellular ribonuclease activities of RNases have been suggested to play an anti-microbial function and to attenuate inflammation upon tissue injury (Rosenberg, 2008; Gupta et al., 2013). In addition to acting extracellularly, RNase A and other superfamily members are internalized via clathrin-dependent endocytosis and macropinocytosis (Chao and Raines, 2011). After internalization, RNases regulate multiple processes, including innate immune responses via endosomal Toll-like receptors and intracellular nucleotide receptors (Gupta et al., 2013; Liu et al., 2013), and induction of apoptosis via the caspase pathway (Chang et al., 2010). Studies also suggest that RNase 3 activates the caspase pathway by forming aggregates on the cell surface without internalization (Navarro et al., 2008, 2010). Thus, these studies indicate that RNase A superfamily members are involved in multiple cellular processes via both ribonuclease activity-dependent and -independent pathways.

Indeed, recent studies further suggested that a ribonuclease activity-independent pathway is critical for the RNase A superfamily to promote cell proliferation. Angiogenin, also known as RNase 5, has been shown to interact with several cellular proteins (Sheng and Xu, 2016; Lyons et al., 2017), including the transmembrane proteins heparan sulfate proteoglycan syndecan-4 (Skorupa et al., 2012), Plexin-B2 (Yu et al., 2017) and EGFR (Wang et al., 2018). The interaction between angiogenin and Plexin-B2 promotes proliferation of mouse embryonic teratocarcinoma P19 cells via activation of the AKT pathway (Yu et al., 2017). Like angiogenin, RNase 4 also promotes proliferation of P19 cells, though it is unclear whether Plexin-B2 is also involved in the action of RNase 4 (Li et al., 2013). In addition to P19 cells, angiogenin and RNase A also trigger cell proliferation of various pancreatic cancer cells via the EGFR-ERK pathway (Wang et al., 2018). Enzymatic dead mutants of RNase A and angiogenin still carry the ability to bind and activate EGFR (Wang et al., 2018). Thus, the abilities of RNase A and angiogenin to promote cell proliferation could be independent of its enzymatic activity. Moreover, promoting cell proliferation is one of common functions of RNase A, angiogenin and RNase 4.

To demonstrate the involvement of endogenous ssRNA in stimulating neuronal Toll-like receptor 7 (TLR7), we previously added RNase A to digest ssRNA in cortical and hippocampal mixed cultures. We found that RNase A treatment neutralizes TLR7-mediated dendritic withdrawal of cultured neurons, because the dendritic length of wild-type neurons, but not *Tlr7*^{-/-} neurons, was increased in the presence of RNase A (Liu et al., 2013). In addition, we noticed that cell density was increased in RNase A-treated cultures. We hypothesized that RNase A treatment promotes cell proliferation of neuronal

cultures. To explore this possibility, here, we investigated whether numbers of proliferating cells are increased in response to RNase A treatment and which types of cells are expanded *in vitro* in the presence of RNase A. Our data suggest that neuronal progenitor cells (NPCs) respond to RNase A. We also examined the involvement of ERK in RNase A downstream signaling. Finally, we demonstrate the effect of RNase A on promoting EdU incorporation *in vivo*. Our study suggests an unexpected activity of RNase A in triggering NPC proliferation.

MATERIALS AND METHODS

Chemicals

RNase A was purchased from Invitrogen (12091-021) and Qiagen (19101). Bovine serum albumin (BSA, A4919), bromodeoxyuridine (BrdU, B5002), cytosine arabinoside (Ara-C, C1768), U0126, and poly-L-lysine (P2636, 30,000-70,000 molecular weight) were purchased from Sigma-Aldrich. EdU (A10044) was purchased from Invitrogen.

Antibodies

Primary antibodies used in this report are summarized in **Table S1**. Alexa Fluor 488- and Alexa Fluor 594-conjugated secondary antibodies were purchased from Invitrogen.

Animals

Wild type C57BL/6 mice were housed in the animal facility of the Institute of Molecular Biology, Academia Sinica, under pathogen-free conditions and a 14 h light/10 h dark cycle with controlled temperature and humidity. Mixed gender embryos were used for neuronal cultures. Adult male mice were used for *in vivo* analysis. All animal experiments were performed with the approval (Protocol Number 13-02-520) of the Academia Sinica Institutional Animal Care and Utilization Committee and in strict accordance with its guidelines and those of the Council of Agriculture Guidebook for the Care and Use of Laboratory Animals.

Primary Culture

Our neuronal cultures were prepared as described previously (Hung et al., 2018). Briefly, cerebral cortices and hippocampi of mouse embryos at E17-18 were dissected, dissociated with trypsin and cultured in Neurobasal/DMEM (1:1) with 2% B27 supplement, 0.5 mM glutamine, and penicillin-streptomycin. EGF and FGF were not included in the medium. RNase A was added at 1 DIV. After treatment for 3 days, cultures were harvested for analysis. Our culture medium contains a final concentration of 2,500 μ g/ml bovine serum albumin (BSA, A4919, Sigma) (Chen et al., 2008). An additional 100 μ g/ml BSA (A4919, Sigma) was added as a negative control for RNase A treatment in this report. We controlled cell density at 2×10^5 cells/well in 12-well plates with 18-mm coverslips precoated with 1 mg/ml poly-L-lysine (P2636, 30,000-70,000 molecular weight, Sigma-Aldrich). These culture conditions enrich the neuronal population. The percentage of glial cells (GFAP⁺ cells) in our cultures is around 2–3% (Liu et al., 2013). To inhibit NPC

proliferation, 1 μ M Ara-C was added to the cultured neurons after 24 h RNase A treatment.

Time-Lapse Imaging

Neurons were cultured with a density of 1.5×10^5 cells/cm² on 36-mm coverslips. Four hours after seeding, neurons were transferred to POC-R cell cultivation system (LaCon) for time-lapse recording. Before recording, neurons were inoculated in LSM510META-NLO system at 37°C with 5% CO₂ supplement for at least 2 h for system balance. The recording was carried out using Plan-Apochromat 20x/NA0.8 M27 objective lens (Carl Zeiss, Inc.) with 0.5% laser energy in a live-cell incubation chamber. Images were acquired every 3 min for 96 h with a resolution of 1,024 \times 1,024 pixels. Results were then processed for publication using ImageJ (NIH) with minimal adjustment of brightness or contrast applied to the whole images.

Neurosphere Culture

NPCs derived from a mixture of mouse cerebral cortices and hippocampi of E17-18 embryos were cultured at a density of 8×10^4 cells/well in flat-bottomed 96-well plates and maintained in F12/DMEM (1:1) with 2% B27 supplement. EGF and FGF were not included in the medium. RNase A or BSA was added to the medium and incubated for 9 days. The cultures were visualized with an Image Xpress Micro system (Molecular Devices) equipped with a 10x objective lens (Plan Fluor; Nikon). The number of neurospheres per well and the area of each neurosphere were measured using software provided by the Image Xpress Micro system. To investigate cell growth of neurospheres in response to different dosages of RNase A, the averaged area of each neurosphere was analyzed for each well. In addition, all neurospheres were divided into nine groups based on their size, ranging from 0-10,000 to >80,000 μ m², using Microsoft Excel software (COUNTIFS function), and the percentage of each group was calculated. Experiments were independently repeated more than three times.

ERK Phosphorylation

At 1 DIV, dissociated neuronal cultures were treated with RNase A (100 μ g/ml) for 0, 10, 20, 30, and 60 min. To investigate the dosage effect of U0126, cultures were treated with U0126 at different dosages (0, 5, or 10 μ M) for 30 min followed by treatment with or without RNase A (100 μ g/ml) for 20 min. For neurosphere cultures, 4 DIV cells were pretreated with U0126 (10 μ M) or DMSO control for 30 min, followed by RNase A (100 μ g/ml) stimulation for 0, 10, 20, 30, and 60 min. Total cell lysates were harvested and subjected to immunoblot analysis using phospho-ERK, pan ERK, and VCP antibodies.

In vitro Labeling of BrdU and Immunofluorescence Staining

BrdU was added to cultured neurons at a concentration of 10 μ M for 2 h before fixation with 4% paraformaldehyde (PFA) and 4% sucrose in phosphate buffered saline (PBS) for 15 min at room temperature. After washing with PBS, cells were denatured with 2N HCl for 30 min at 37°C. Cells were then

washed twice with PBS and permeabilized with 0.1% Triton-X 100 (Sigma-Aldrich) in PBS for 10 min at room temperature and blocked with 5% BSA (A7906; Sigma-Aldrich) in PBS for 30 min. Fixed cells were incubated with primary antibodies diluted in 5% BSA/PBS overnight at 4°C. After washing with PBS, neurons were incubated with Alexa Fluor-488- and 594-conjugated secondary antibodies for 2 h at room temperature. Samples were then mounted with Vectashield mounting medium (H-1000; Vector Laboratories) and visualized with an Axio Imager-Z1 or M2 microscope (Carl Zeiss). To quantify the effect, five images were captured randomly and blindly from each coverslip under a 10x objective lens/NA 0.45 or 20x objective lens/NA 0.8 (Plan Apochromat; Carl Zeiss). The average of five images represented the result of each coverslip. For the Z1 microscope, immunofluorescence images were captured with a digital AxioCam MRm camera driven by the digital image processing software AxioVision.

Stereotactic Brain Surgery and Intracerebroventricular Injection

Three-month-old male C57BL/6 mice were deeply anesthetized with zoletil (0.25 mg/kg bodyweight) and xylazine (0.08 mg/kg bodyweight) in 0.9% NaCl. Mice were stereotactically implanted with a stainless steel guide cannula (outer diameter 0.55 mm/inner diameter 0.31 mm/length 8 mm) into the right lateral cerebroventricle (0.54 mm posterior to the bregma, 1.2 mm lateral to midline and 2.21 mm below the skull). Three screws fixed the guide tube to the skull and dental cement was used to encase the screws and guide tube. After two weeks of recovery, BSA (90 μ g/ μ l) or RNase A (90 μ g/ μ l; QIAGEN) was dissolved in artificial cerebrospinal fluid (aCSF) with 0.01% Fast Green and injected into the lateral cerebroventricle at a volume of 2 μ l for 10 min (rate 0.2 μ l/min) under anesthesia with 2.5% isoflurane. The injector was removed 10 min later.

EdU *in vivo* Labeling And Quantification

After intracerebroventricular injection of BSA or RNase A (1-4 times), each group of mice received a single intraperitoneal injection of EdU (stock: 10 mg/ml in 10% DMSO) at a dosage of 100 mg/kg bodyweight to monitor cell proliferation. Mouse brains were harvested 8 days after injection of BSA or RNase A. After perfusion with PBS and 4% PFA/PBS, brains were dissected and postfixed with 4% PFA/PBS overnight at 4°C. Fifty- μ m-thick coronal sections were sliced with a LEICA VT 1200S microtome. EdU staining was conducted using the Click-iT™ Plus EdU Imaging kit with Alexa Fluor 488 (C10637; Invitrogen) according to the manufacturer's instructions. Brain sections were permeabilized with 0.5% Triton X-100 in PBS for 30 min. After washing twice with 3% BSA in PBS, brain sections were incubated with a Click-iT™ reaction cocktail for 30 min while protected from light. The sections were washed twice with 3% BSA in PBS and mounted with DAPI in Vectashield mounting medium (H-1000; Vector Laboratories). Samples were visualized with an Axio Imager M2 microscope (Carl Zeiss) equipped with a 10x objective lens/NA 0.45 (Plan Apochromat; Carl Zeiss). Fluorescence images were captured with a digital Rolera EM-C² camera driven by the digital image processing software Zen Blue.

All images were converted into 8-bit (**Figures S2A, S3A**) and adjusted with a threshold (“Moments” and “B&W” modes in “Dark background”) (**Figures S2B, S3B**) using ImageJ software. The area of fluorescence reactivity was analyzed using “Analyze Particles” with the setting of 30-infinity pixel units and 0.01–1.00 circularity (**Figures S2C, S2D, S3C–E**). The quantitative results were manually corrected to remove artifacts, such as high background or false signals (**Figures S2E, S3F**). The data were then transferred to Excel to calculate the ratio of number of EdU puncta to total area of brain at the lateral ventricle (**Figures S2E,F**) or both sides of the hippocampus (**Figure S3B**), as well as the percentage area of EdU signal. Examples of the quantification process are available in **Figures S2, S3**.

In vivo Labeling of BrdU and Immunofluorescence Staining

After intracerebroventricular injection of BSA or RNase A, each group of mice received intraperitoneal injection of BrdU (stock: 10 mg/ml in 10% DMSO) at a dosage of 50 mg/kg bodyweight, as indicated in **Figure 9A**. Mouse brains were harvested 30 days after injection of BSA or RNase A. After perfusion with PBS and 4% PFA/PBS, brains were dissected and postfixed with 4% PFA/PBS overnight at 4°C. For BrdU staining, sections were denatured with 2N HCl for 30 min at 37°C. After washing twice with PBS, brain sections were permeabilized with 0.5% Triton-X 100 (Sigma-Aldrich) in PBS for 10 min at room temperature and blocked with blocking solution (1% BSA, 3% horse serum, and 0.3% Triton-X 100 in PBS) for 30 min. The sections were then incubated with the anti-BrdU antibody (ab6326, Abcam) and other primary antibodies diluted in blocking solution overnight at 4°C. After washing with PBS, the sections were incubated with Alexa Fluor-488- and 594-conjugated secondary antibodies (1:500) for 2 h at room temperature. The sections were then washed twice with PBS and mounted with DAPI in Vectashield mounting medium (H-1000; Vector Laboratories). Samples were visualized with an Axio Imager M2 microscope (Carl Zeiss) equipped with a 10x objective lens/NA 0.45 (Plan Apochromat; Carl Zeiss) and a confocal microscope (LSM 700; Carl Zeiss) equipped with a 20x/NA 0.8 (Plan-Apochromat; Carl Zeiss) objective lens.

Statistical Analysis

For culture, each set of experiment was independently repeated 3–4 times using different litters. For each experiment, five fluorescence images were captured randomly and blindly from each coverslip. The average of the data of five images represented the result of each coverslip. All graphs were plotted and analyzed using GraphPad Prism 5.0 or 7.0. Data are presented as the mean plus SD. *P* values of <0.05 were considered significant. In **Figures 7A,B**, the experiment was repeated three times using independent neuronal culture. The band intensity of p-ERK and ERK in each sample was quantitated using imageJ. After obtained p-ERK/ERK ratio in each sample, all the p-ERK/ERK ratios were further normalized to the control. For multiple group comparisons, we applied the one-way analysis of variance (ANOVA) or two-way ANOVA with Bonferroni’s test. For two group comparisons, the normality of each group

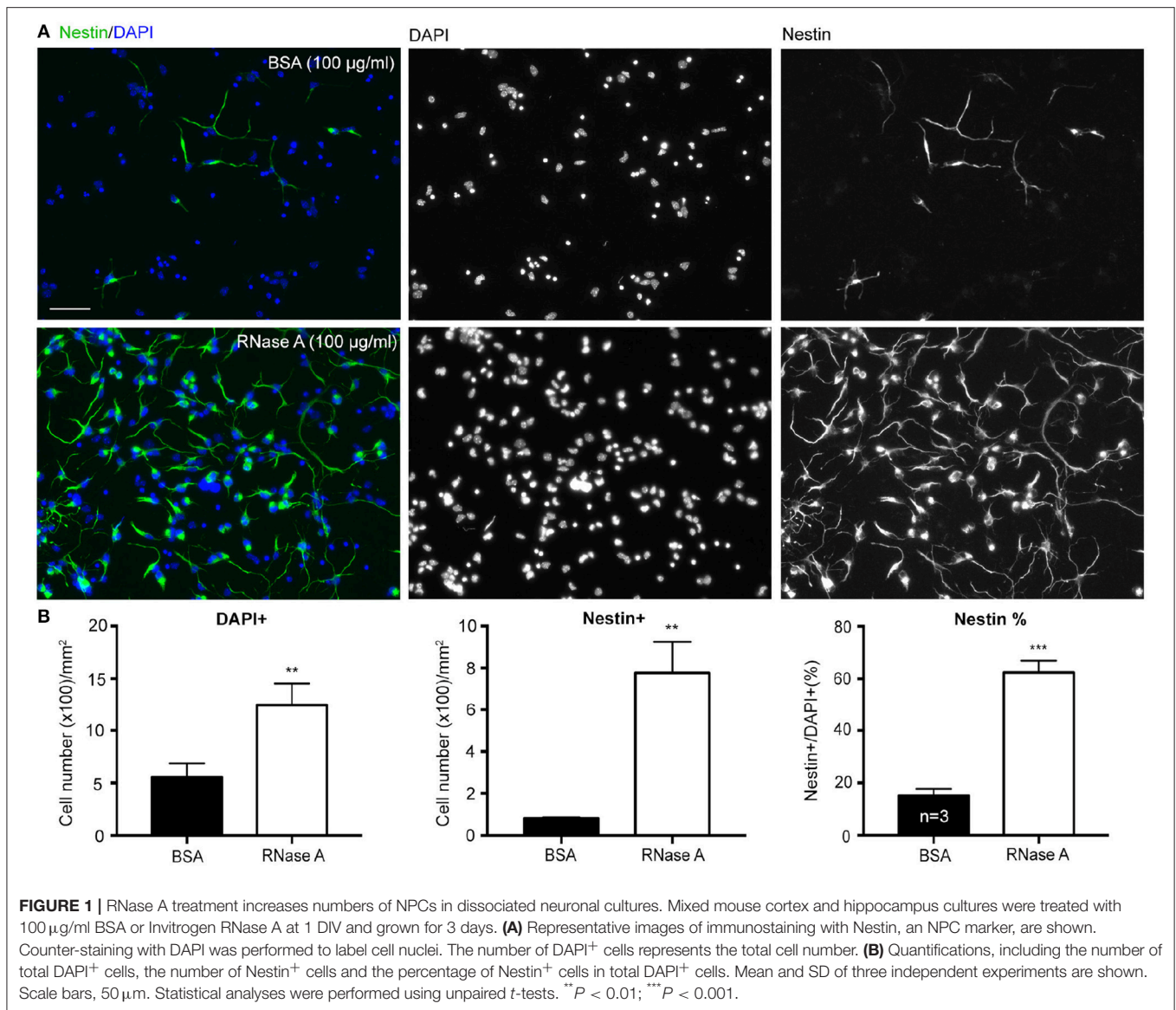
was analyzed using a Shapiro-Wilk normality test. Statistical analysis of the normally distributed groups was performed using unpaired *t*-tests. Statistical analysis of non-normally distributed groups was performed using two-tailed nonparametric tests (Mann-Whitney tests). The variance between groups was not statistically compared. Data collection and analysis were conducted randomly and blind through relabeling of the samples by other lab members.

RESULTS

RNase A Increases Cell Number of NPCs in Dissociated Neuronal Cultures

To confirm the role of ssRNA in regulation of neuronal morphology, RNase A was added to cortical and hippocampal mixed neuronal cultures to digest ssRNA in cultures (Liu et al., 2013). In addition to promoting dendritic outgrowth (Liu et al., 2013), we noticed when RNase A (final concentration 100 µg/ml) purchased from Invitrogen was added to cortical and hippocampal mixed neuronal cultures at 1 day *in vitro* (DIV), the cell density indicated by DAPI counter-staining was increased at 4 DIV (**Figures 1A,B**). Our cultures were dissociated neuronal cultures grown in Neurobasal/DMEM medium with B27 supplement (Hung et al., 2018). BSA (final 2,500 µg/ml) was the major protein component in the medium (Chen et al., 2008). Thus, we first used an additional 100 µg/ml of BSA as a negative control for RNase A treatment. Compared with BSA control, RNase A increased total cell number by more than 200% (**Figure 1B**). Immunostaining using Nestin antibody showed that the number of Nestin⁺ cells was noticeably increased in RNase A-treated groups (**Figures 1A,B**), suggesting an increase of NPC number upon RNase A treatment. The increased number of NPCs was roughly equal to the increased total cell number (**Figure 1B**, left vs. middle). When we calculated the percentage of Nestin⁺ cells, we also found that the population of Nestin⁺ cells increased from ~20% in BSA groups to 60% in RNase A-treated groups (**Figure 1B**, right). Thus, compared with BSA control, RNase A treatment increased the population of Nestin⁺ NPCs in dissociated neuronal cultures.

Since our culture medium was originally designed for neuronal culture (see Materials and Methods), we did not expect to find Nestin⁺ NPCs under our culture conditions. To confirm that the observed cells were NPCs, we also performed immunostaining with SOX2 antibody, another NPC marker. Indeed, Nestin and SOX2 co-existed in the same cells (**Figure 2A**), supporting that the proliferated cells are NPCs. If NPCs are indeed present in our cultures, we would expect to see dividing cells in our cultures. To assess this possibility, we conducted time-lapse recording from DIV 0 to 4. We found that dividing cells were easily visible in our neuronal cultures. We present an example containing three NPCs in a single field in **Figure 2B** and **Movie S1**. One of the NPCs underwent a single division and differentiated into neurons (**Figure 2B**, blue asterisk). Two NPCs underwent several divisions and produced multiple daughter cells (**Figure 2B**, red

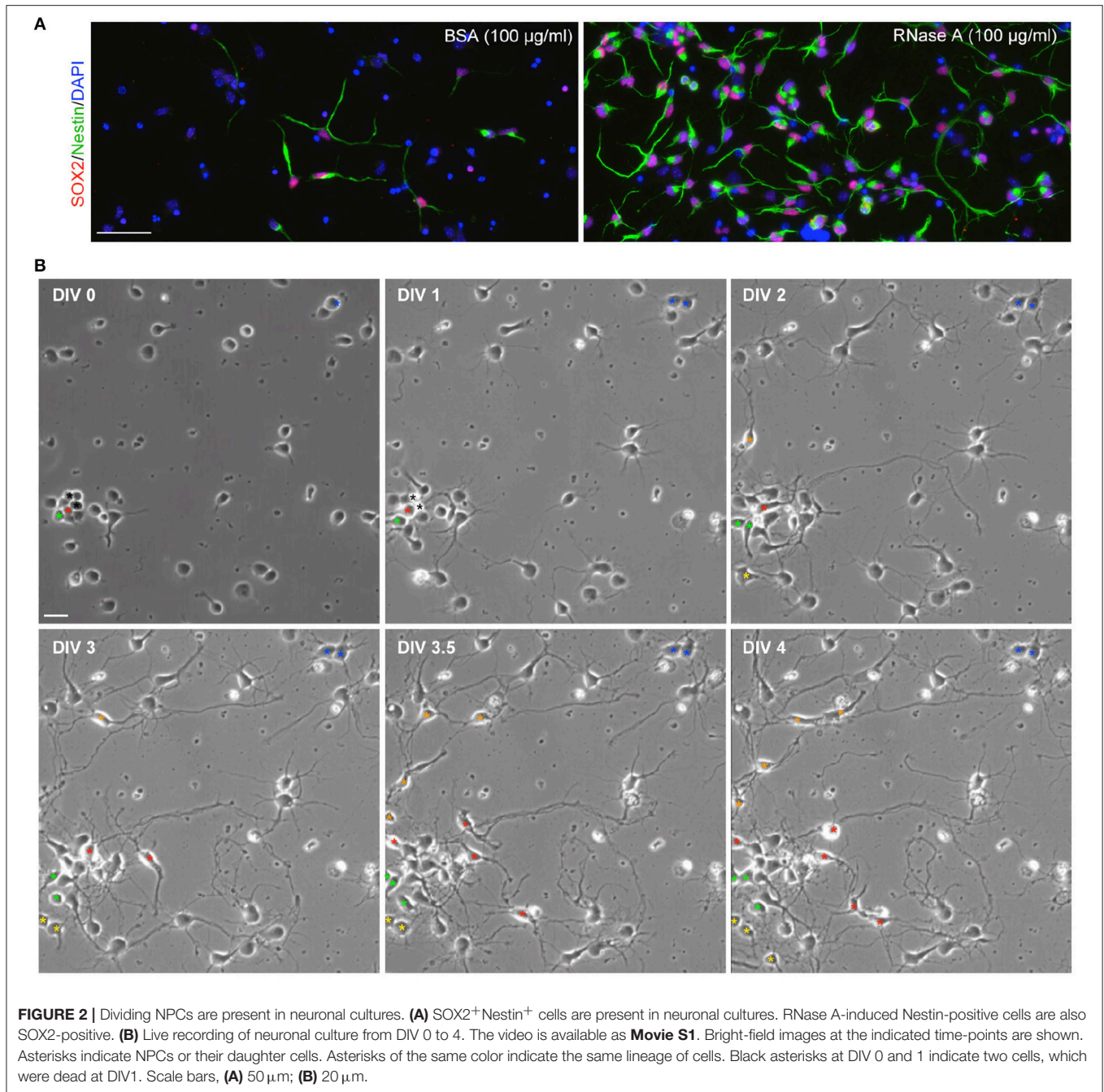


and green asterisks). These NPCs typically had two or three long thick processes and exhibited highly motile nuclei moving along their processes (**Movie S1**). The morphology of these dividing cells is similar to the Nestin⁺ cells revealed by immunostaining (**Figure 1**). These data suggest that Nestin- and SOX2-positive dividing NPCs are present in our neuronal cultures.

To further confirm the effect of RNase A on NPC proliferation, we tested RNase A purchased from different company, namely Qiagen. Similar to RNase A from Invitrogen (**Figure 1**), Qiagen RNase A also increased NPC population in neuronal cultures, as the percentage of Nestin⁺ NPCs in total cells was increased by RNase A compared to BSA control (**Figures 3A,B** upper). Thus, both Invitrogen and Qiagen RNase A increased NPC number in cultures compared with BSA control.

In addition to BSA control, mock control without adding extra protein was also included (**Figure 3**). It was clear that the population of Nestin⁺ cells in BSA treated group was comparable to mock control and that RNase A treatment increased the percentage of Nestin⁺ cells compared with mock control (**Figure 3B**, upper). Thus, no matter comparing with mock control or BSA control, RNase A treatment noticeably increases the population of Nestin⁺ cells in dissociated neuronal cultures.

We also performed a double staining using antibodies against Nestin and MAP2, a neuronal marker (**Figure 3**). Neurons and NPCs are the two major populations in our cultures. Compared with BSA and mock controls, we found that the population of Nestin⁺ cells was increased from ~20% to ~40–70% of total Nestin⁺ and MAP2⁺ cells (**Figure 3B**). Thus, the population of Nestin⁺ cells was increased upon RNase A



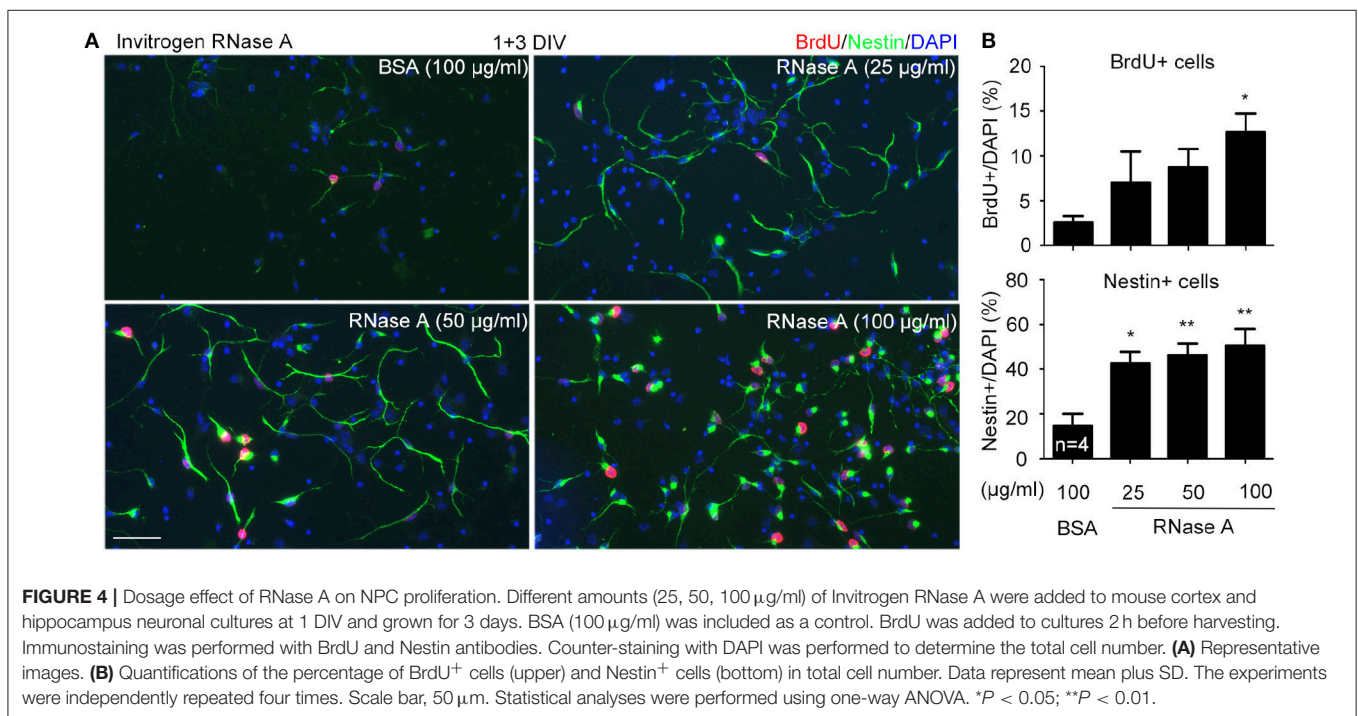
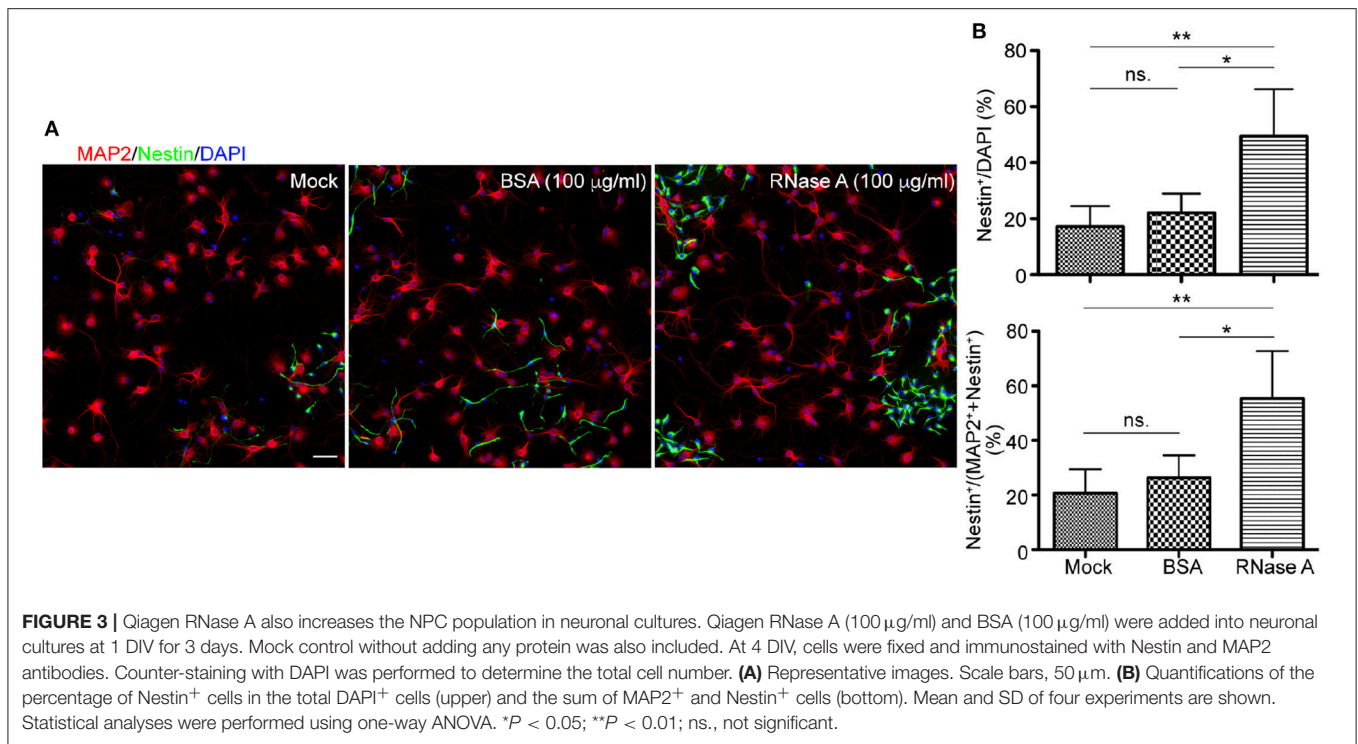
treatment no matter we used DAPI staining to count the total cell number or the sum of Nestin⁺ and MAP2⁺ cells to represent the major populations in cultures.

RNase A Promotes NPC Proliferation

Increased NPC population in our cultures suggests that RNase A treatment likely promotes proliferation. To test the effect of RNase A on NPC proliferation, we added 5-bromo-2'-deoxyuridine (BrdU, a thymidine nucleoside analog) into cultures 2 h before harvesting. Meanwhile, the dosage effect of

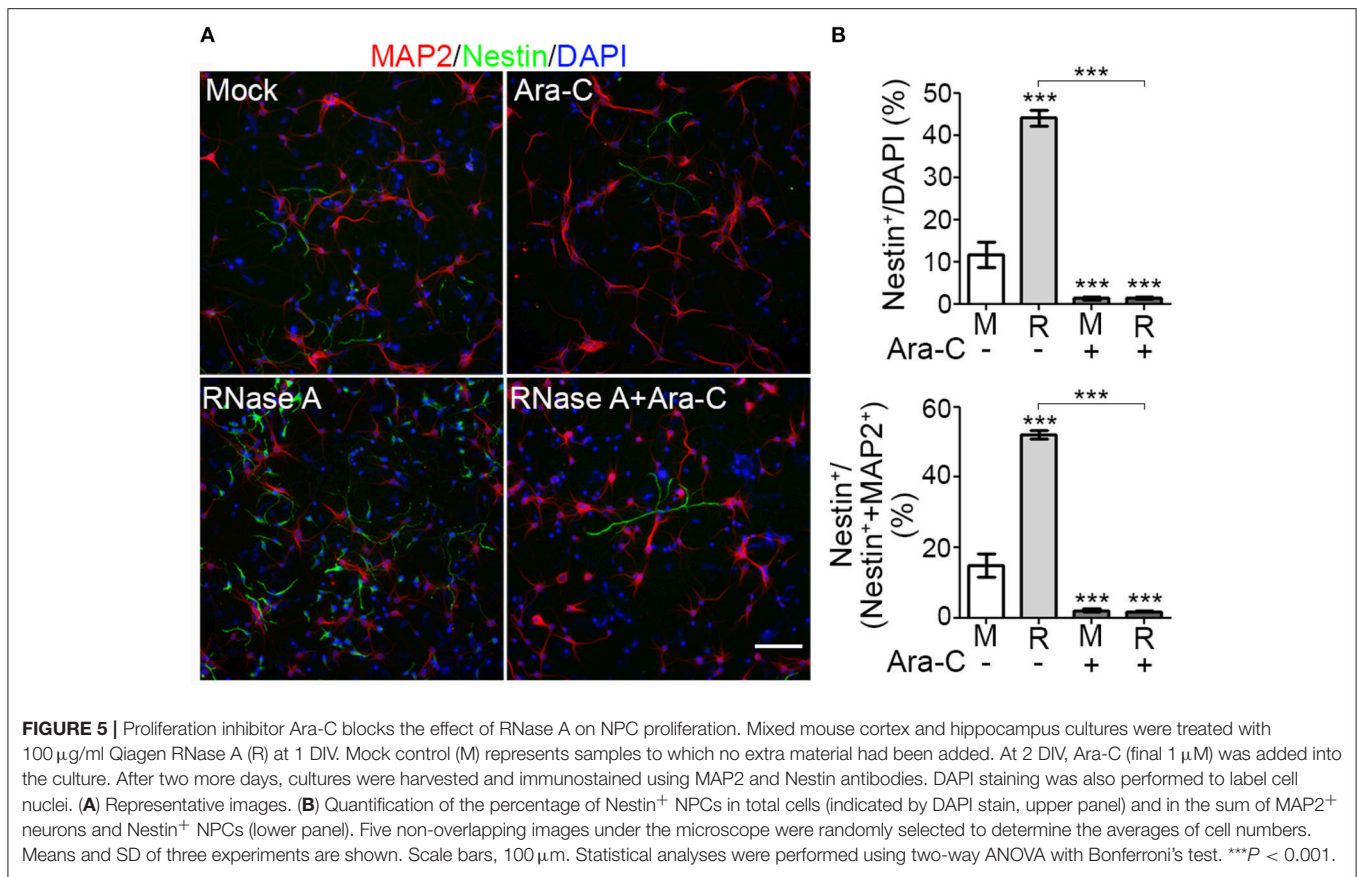
RNase A was also investigated. We found that similar to the effect on Nestin⁺ cells, RNase A treatment indeed increased the population of BrdU⁺ cells (**Figures 4A,B**). Twenty five µg/ml RNase A was sufficient to increase the population of Nestin⁺ cells (**Figures 4A,B**). It also increased BrdU labeling in the cultures, though the difference was not yet significant. These data suggest that RNase A treatment promotes BrdU incorporation by NPCs.

To reinforce the evidence for an effect of RNase A on NPC proliferation, we added the proliferation inhibitor cytosine arabinoside (Ara-C) to our cultures. Compared with



mock control, RNase A treatment increased the percentage of Nestin⁺ cells from <20% to ~44% of total cells (indicated by DAPI staining) and ~52% of the sum of MAP2⁺ neurons and Nestin⁺ NPCs (Figures 5A,B). Addition of 1 µM Ara-C efficiently reduced the numbers of Nestin⁺ cells in both

control and RNase A-treated cultures (Figure 5B). Whenever we added Ara-C to cultures, the percentage of Nestin⁺ NPCs was reduced to ~2% that of total cells or the sum of MAP2⁺ neurons and Nestin⁺ NPCs (Figure 5B). Taken together, the results of our BrdU incorporation assay and Ara-C inhibition



experiment indicate that RNase A treatment promotes NPC proliferation.

RNase A Also Increases Neurosphere Cell Mass

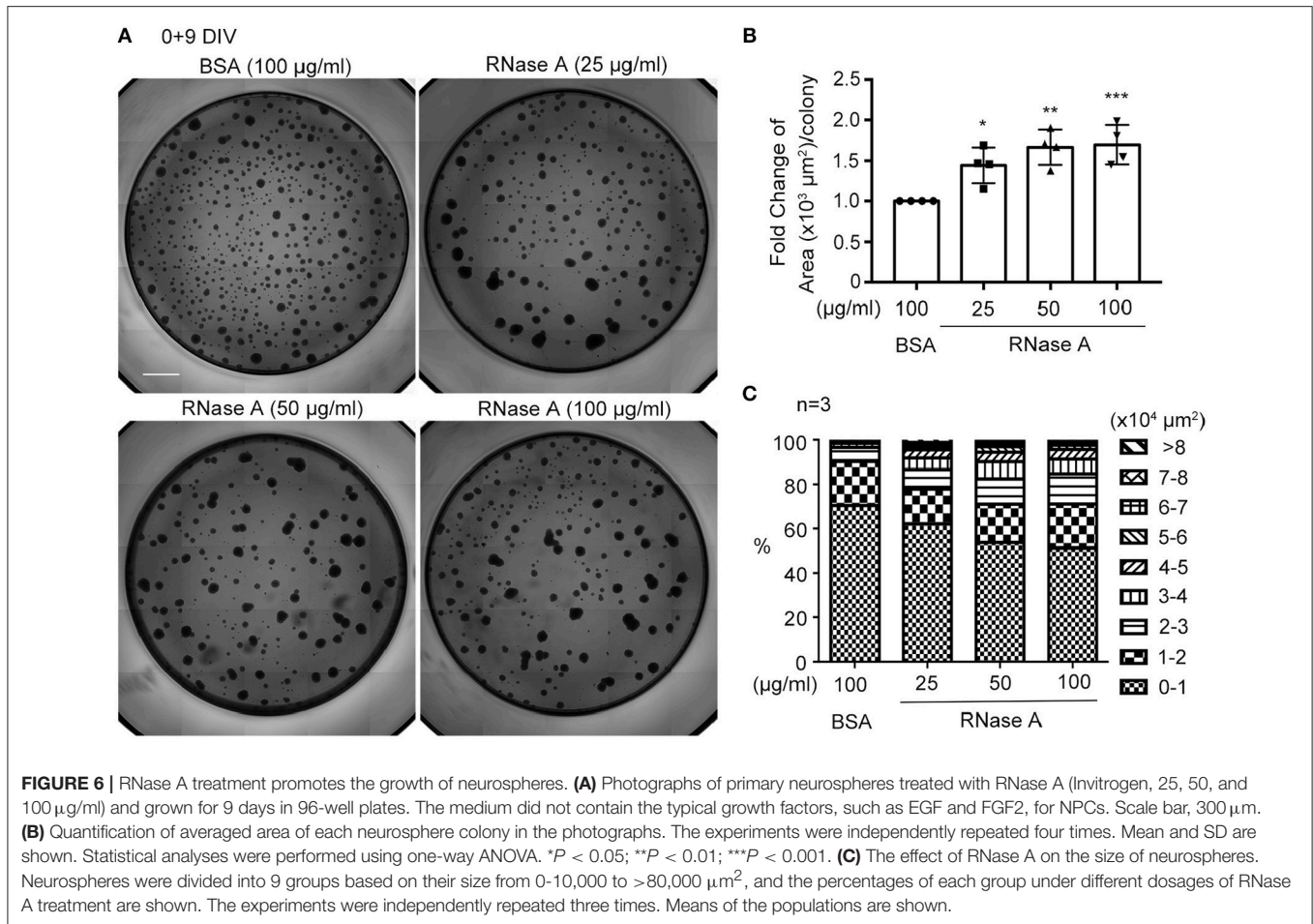
We utilized dissociated neuronal cultures for all of the previously described analyses. We then examined the effect of RNase A on neurosphere cultures. Different amounts of RNase A (25, 50, or 100 $\mu\text{g/ml}$) were added to neurosphere cultures in the absence of EGF and FGF2 (Figures 6A–C). Nine days after culture, the averaged area of each neurosphere had increased in a dosage-dependent manner in the 25–100 $\mu\text{g/ml}$ RNase A-treated groups (Figure 6B). We also quantified the populations of differently sized neurospheres and found that the numbers of larger colonies had increased in the presence of RNase A (Figure 6C). Thus, RNase A also promotes the growth of neurospheres.

ERK Activation Is Involved in RNase A-Mediated Neurogenesis

A very recent study showed that RNase A and angiogenin activate the EGFR-ERK pathway and AKT to promote proliferation of pancreatic cancer cells (Wang et al., 2018). We wondered whether RNase A also activates these pathways in NPCs. To investigate this possibility, we monitored ERK activity (indicated by ERK phosphorylation levels) upon RNase A treatment. In dissociated cortical and hippocampal neurons,

phospho-ERK signals were increased 10 min after RNase A treatment and lasted for at least 60 min (Figure 7A). To confirm that the increased ERK phosphorylation was specifically caused by activation of the ERK pathway, we added U0126 (a MEK1/2 inhibitor) to the culture 30 min before RNase A treatment. Indeed, U0126 effectively eliminated RNase A-induced ERK phosphorylation in dissociated cortical and hippocampal neurons (Figure 7B). We also investigated the involvement of ERK in the response of neurospheres to RNase A. As for dissociated cultures, RNase A treatment increased ERK activity in neurospheres (Figure 7C, left panel), and U0126 treatment blocked the ERK activity induced in them by RNase A (Figure 7C, right panel). We also examined the activity of AKT upon RNase A treatment. In contrast to ERK, AKT activation upon RNase A stimulation was not obvious (Figure S1). Thus, our evidence suggests that RNase A treatment activates the ERK pathway but does not promote AKT activity.

To further investigate the role of ERK in RNase A-dependent neurogenesis, we monitored the effect of U0126 on the number of Nestin⁺ cells upon RNase A treatment. Different doses of U0126 (0, 2, 5, 10, or 20 μM) were added to dissociated cultures 30 min before adding RNase A or BSA at 1 DIV. Three days later, the cultures were immunostained with Nestin and MAP2 antibodies and counter-stained with DAPI to determine their populations of Nestin⁺ cells. Consistent with its effect of reducing ERK



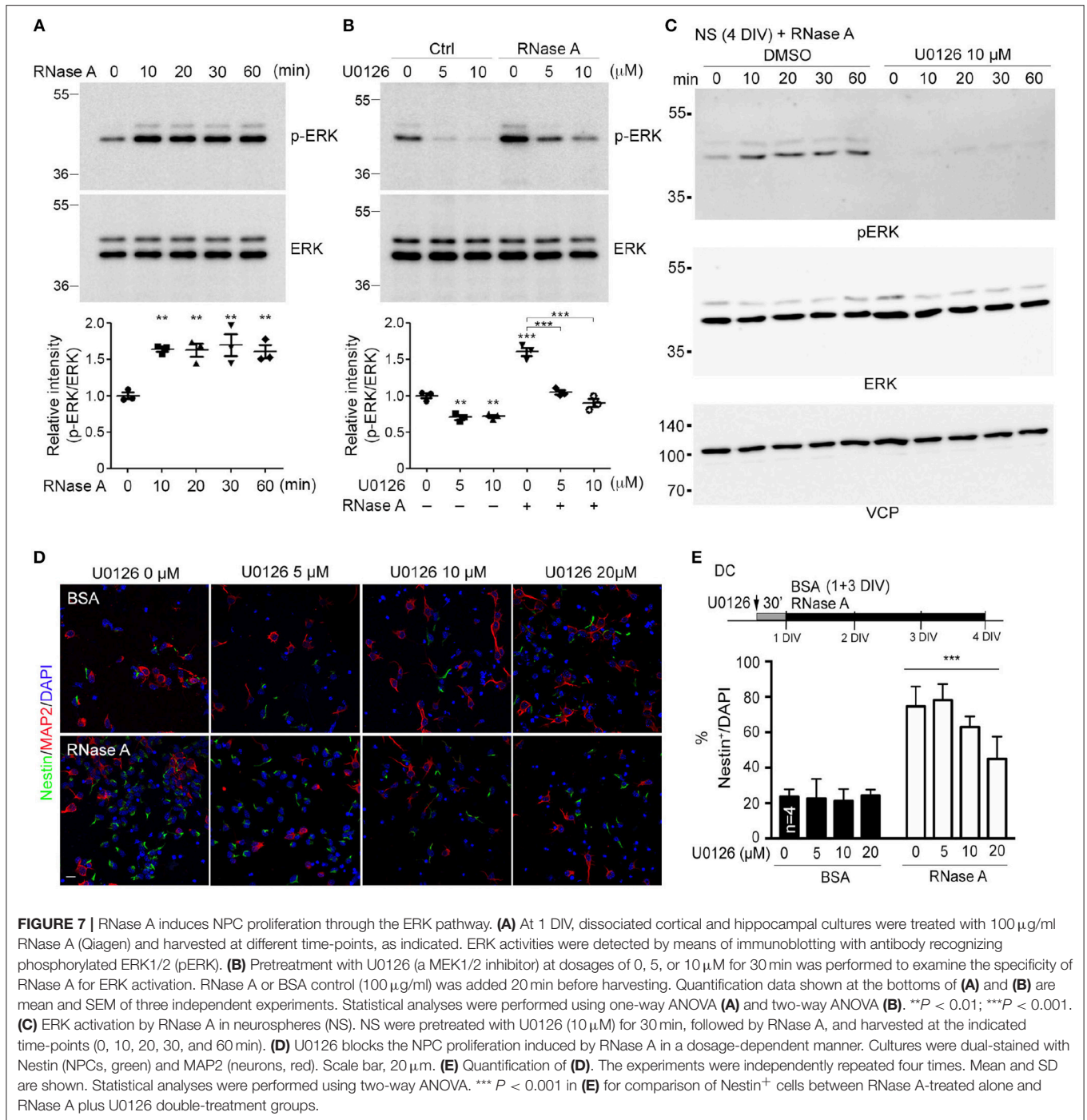
phosphorylation, U0126 exhibited the dosage-dependent effect of decreasing the numbers of Nestin⁺ cells induced by RNase A (Figures 7D,E). These results suggest that RNase A treatment induces ERK activation and promotes NPC proliferation in cultures.

RNase A Promotes NPC Proliferation in Mouse Brains

We then investigated whether RNase A is able to promote NPC proliferation in mouse brains. RNase A was injected daily into one of the lateral ventricles of mouse brains for 1, 2, 3, or 4 days. After the last dose of RNase A, the thymidine nucleoside analog 5-ethynyl-2'-deoxyuridine (EdU) was intraperitoneally injected into mice to label dividing cells. Four doses of BSA (BSA x4) were performed as a control. Mice were then sacrificed to monitor EdU signals at day 8, i.e., 7 days after the first shot of RNase A or BSA had been injected (Figures 8A,B). Since RNase A was injected into lateral ventricle, we expected to find more EdU-positive cells at subventricular zone in RNase A treated mice. Indeed, compared with the BSA control (BSA x4), the four injections of RNase A (RNase A x4) noticeably increased EdU puncta in periventricular zone (Figure 8C). Two parameters

were measured to quantify the effect of RNase A on neurogenesis. We first measured the total numbers of EdU⁺ nuclei. Since some EdU⁺ cells tended to aggregate, it was difficult to count individual cells. Therefore, as a second measure, we established the areas of EdU signal. Compared with BSA controls, both parameters indicated that the four doses of RNase A increased EdU labeling in mouse brains (Figures 8C-E). In terms of a dosage effect, either three or four doses (but not one or two) of RNase A noticeably increased EdU signals (Figures 8F,G). Thus, our results suggest that, similar to the results for neuronal cultures, intracerebroventricular injection of RNase A promotes NPC proliferation *in vivo*.

Although RNase A was injected into the lateral ventricle, we noticed that EdU-positive cells were not restricted to the subventricular zone. Instead, they were distributed over the entire hippocampus and in other brain regions (Figures 8C-G). It seems that the EdU-positive cells could migrate from the subventricular zone into other brain regions. To further assess this behavior, we modified our *in vivo* labeling experiments by injecting more BrdU and monitoring the distribution of BrdU-positive cells a month later (Figure 9A). In the BSA control group, we found very few BrdU-positive cells, and they were concentrated in the subgranular zone of the dentate gyrus



and the region surrounding the lateral ventricle (**Figure 9B**, upper). In the RNase A group, we observed numerous BrdU-positive cells in the hippocampus, amygdala, cortex, thalamus, and striatum (**Figure 9B**). These BrdU-positive cells were Nestin- and GFAP-positive (**Figure 9C**), but Iba1-negative (**Figure S4**), suggesting that they are a lineage of NPCs but not microglial cells. We noticed that Nestin proteins were highly

concentrated in the nuclei of BrdU-positive cells (**Figure 9C**), consistent with a recent report indicating that nuclear Nestin is involved in preventing cell senescence (Zhang et al., 2018). These data suggest that RNase A-induced NPCs are able to migrate to various brain regions and they further support the role of RNase A in promoting NPC proliferation and maintenance.

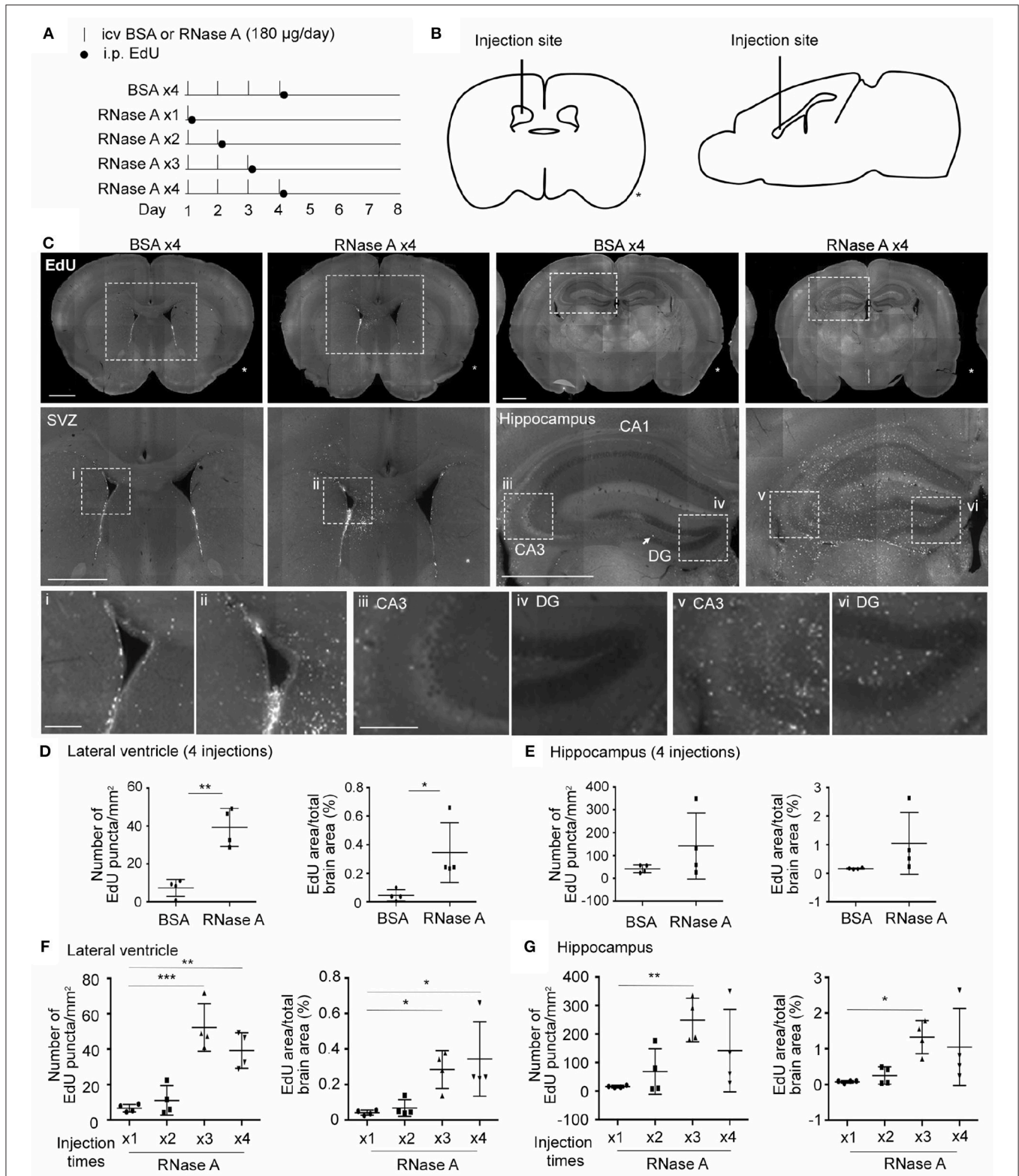
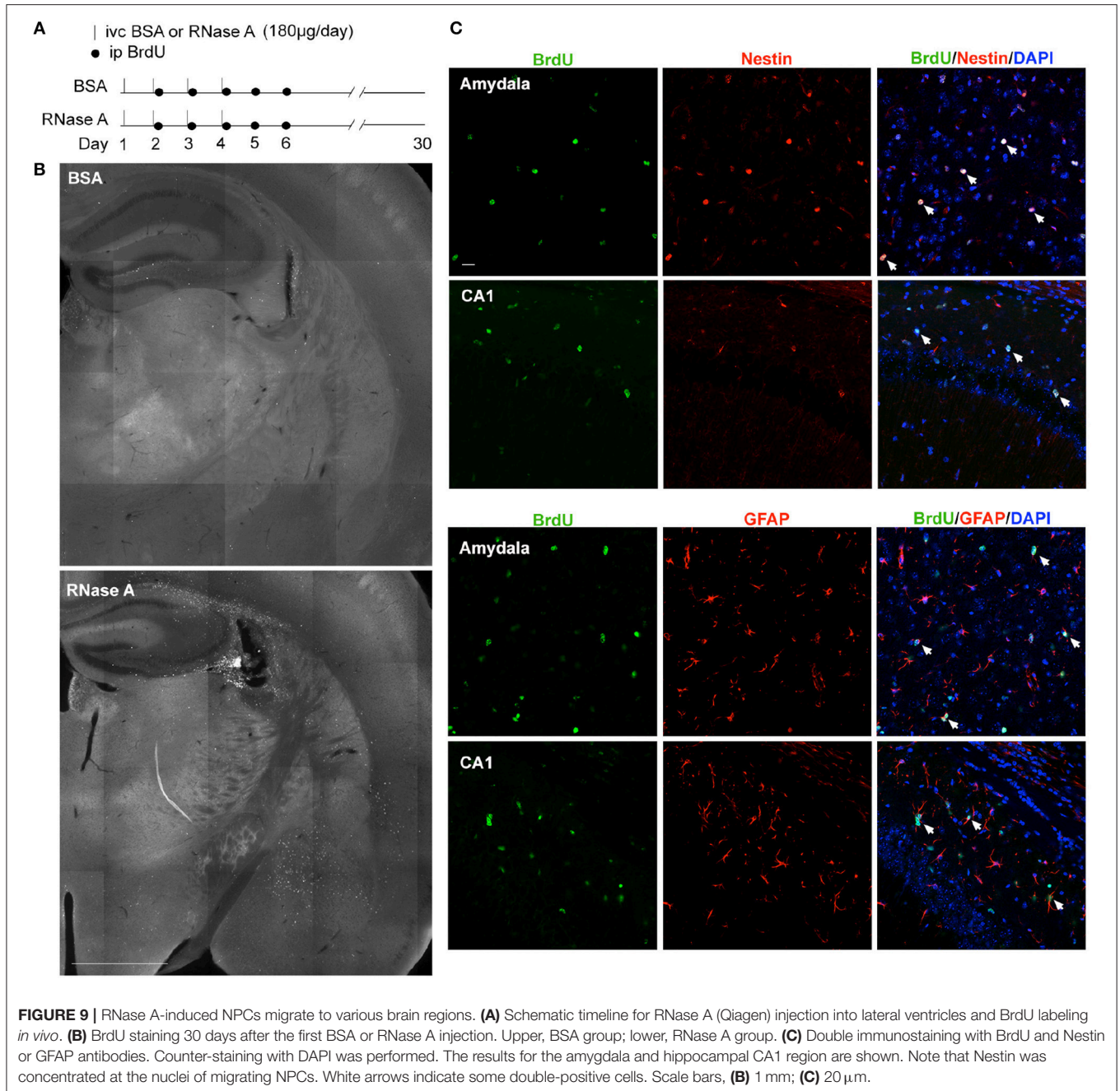


FIGURE 8 | RNase A treatment induces EdU incorporation in mouse brains. **(A)** Schematic timeline for RNase A (Qiagen) treatment and EdU labeling. Intracerebroventricular (icv) injection of 180 µg RNase A or BSA control was performed once per day for one to four days, as indicated. After the last injection of each group, mice received a single intraperitoneal (i.p.) injection of EdU (100 mg/kg) to label proliferated cells. Mouse brains were harvested at day 8 after the first icv injection. **(B)** Schematic diagram showing the position of the icv injection. * indicates the non-injected side. **(C)** Representative images of EdU labeling of the BSA x4 (Continued)

FIGURE 8 | and RNase A x4 groups in the subventricular region of the lateral ventricle (SVZ) and hippocampus. Images in the middle panel of **(C)** are enlargements of the squares in the respective upper panel; scale bar, 1 mm. Arrow points a EdU-positive cell at subgranular zone of dentate gyrus. Bottom panel of **(C)**; images (i, ii: SVZ; iii, v: zone CA3 of hippocampus; iv, vi: dentate gyrus, DG) are enlargements of the squares in the middle panels; scale bar, 200 μ m. **(D–G)** Quantification of EdU-positive cells in both sides of the **(D, F)** lateral ventricle and **(E, G)** hippocampus. The same datasets of RNase A x4 are used in **(D, F)** and **(E, G)**. Data represent mean \pm SD ($n = 4$ mice per group). * $P < 0.05$; ** $P < 0.01$; *** $P < 0.001$. **(D, E)** Unpaired *t*-test or Mann-Whitney test; **(F, G)** One-way ANOVA.



DISCUSSION

We unexpectedly found that RNase A can trigger NPC proliferation. RNase A purchased from either Invitrogen or Qiagen promotes BrdU incorporation and increases numbers of

NPCs in dissociated neuronal cultures as well as neurosphere cell mass. Ara-C treatment assay further suggests that the effect of RNase A on NPCs is to enhance proliferation. Our study also indicates that the ERK pathway is critical for the effect of RNase A on NPC proliferation. Addition of U0126 to inhibit the

ERK pathway efficiently neutralized the triggering effect of RNase A on NPC proliferation. Finally, we have also demonstrated that local infusion of RNase A into mouse cerebroventricles noticeably promotes EdU incorporation, reflecting entry of cells into S phase, *in vivo*. Thus, RNase A possesses an unexpected function of triggering NPC proliferation both *in vitro* and *in vivo*.

Studies have shown that cell surface receptors, including the transmembrane proteins heparan sulfate proteoglycan syndecan-4 (Skorupa et al., 2012), Plexin-B2 (Yu et al., 2017), and EGFR (Wang et al., 2018), are involved in the binding, internalization, and signaling of RNase A and angiogenin, another member of the RNase A superfamily (Chao and Raines, 2011; Gupta et al., 2013; Yu et al., 2017; Wang et al., 2018). EGFR is the common cell surface receptor of RNase A and angiogenin to trigger proliferation of pancreatic cancer cells (Wang et al., 2018). Bovine RNase A binds to EGFR and transmits EGFR downstream signaling, including ERK activation, in various types of cancer cells (Wang et al., 2012). Since the EGFR pathway is also well-known to promote neurogenesis (Mahanthappa and Schwarting, 1993; Ferri and Levitt, 1995; Wong and Guillaud, 2004), it is likely that the EGFR pathway is involved in the effect of RNase A on promoting NPC proliferation. ERK activation by RNase A treatment in neuronal cultures echoes this speculation. Moreover, the cancer cell study showed that the enzymatic activity of RNase A is not involved in the proliferation of cancer cells (Wang et al., 2018), so if RNase A uses the same mechanism to promote NPC proliferation, its enzymatic activity may not be critical for its effect. We found that ERK activity was increased 10 min after RNase A treatment. It is likely that RNase A binds to a EGFR and then activates an ERK pathway. In addition to activation of cell surface receptor, members of the RNase A superfamily are known to influence innate immune responses through RNA degradation and consequent regulation of RNA-binding TLRs or other nucleotide sensors in cells (Gupta et al., 2013; Liu et al., 2013; Chen et al., 2014). In particular, it has previously been suggested that TLR3 plays a role in neurogenesis (De Miranda et al., 2010; Okun et al., 2010; Forrest et al., 2012). Although TLR3 preferentially binds dsRNA, it can still recognize incomplete stem structures in viral ssRNA (Tatematsu et al., 2013). Thus, RNase A degradation of ssRNA might influence the activity of TLR3. Indeed, in a study of myocardial ischemia-reperfusion injury, RNase A was shown to reduce serum RNA levels and to attenuate TLR3 activation in the injury pathway (Chen et al., 2014). It would be interesting to explore further whether the innate immune receptors play a role in RNase A-mediated NPC proliferation. Enzymatic activity-dependent and -independent pathways do not mutually exclude from each other. It will be intriguing to explore the possibility in the future.

We used bovine RNase A to stimulate NPC proliferation. The bovine and human orthologs of RNase A (a rapidly evolving gene) share ~70% amino acid sequence identity. It is unclear whether RNase A from humans or other species

also triggers NPC proliferation. Nevertheless, another two members of the RNase A superfamily, namely RNase 4 and angiogenin, also possess the ability to promote cell proliferation (Li et al., 2013; Yu et al., 2017). Apart from promoting cell proliferation, recent studies have indicated that members of the RNase A superfamily have cytotoxic and anti-tumor activities. *Rana catesbeiana* RNase A induces cell death of human glioblastoma cell lines (Chen et al., 2015). Intramuscular injection of RNase A suppresses growth and metastasis of transplanted murine Lewis lung carcinoma in mice (Mironova et al., 2013, 2017). Use of mutated human RNases as anti-tumor drugs has been suggested (Suzuki et al., 1999; Attery et al., 2018). However, our results and a recent study (Wang et al., 2018) evidence a role of bovine RNase A in promoting proliferation of NPCs and various cancer cells, suggesting that RNase A exhibits versatile activities in different cell types and also that different RNases have differing biological activities. Thus, caution should be exercised when applying RNases, particularly *in vivo*.

AUTHOR CONTRIBUTIONS

H-YL designed and performed the majority of experiments, blind analyzed the data, and wrote the manuscript. C-YC designed and performed the experiments of Ara-C inhibition and ERK phosphorylation and wrote the manuscript. Y-FH, H-RL, and T-NH performed and assisted with the *in vivo* experiment. H-WC performed the time-lapse recording to monitor NPC proliferation and wrote the manuscript. W-PL contributed mock control experiment and wrote the manuscript. C-NC and P-YS assisted with biochemical analysis. Y-PH designed experiments, supervised the project, secured financial support, and wrote the manuscript. All authors read and approved the final version of manuscript.

ACKNOWLEDGMENTS

This work was supported by grants from Academia Sinica (AS-IA-106-L04) and the Ministry of Science and Technology (MOST 107-2321-B-001-011 and 105-2311-B-001-061-MY3) to Y-PH. We thank Dr. Ting-Fang Wang for critical discussion and technical support, Dr. Shu-Yun Tung at the Genomics Core, Ms. Sue-Ping Lee at the Imaging Core and Dr. Yu-Jie Chen at Institute of Molecular Biology, Academia Sinica, for technical support and members of Dr. Yi-Ping Hsueh's laboratory for relabeling samples for blind experiments and technical assistance, and Dr. John O'Brien for English editing.

SUPPLEMENTARY MATERIAL

The Supplementary Material for this article can be found online at: <https://www.frontiersin.org/articles/10.3389/fnmol.2018.00428/full#supplementary-material>

REFERENCES

- Attery, A., Dey, P., Tripathi, P., and Batra, J. K. (2018). A ribonuclease inhibitor resistant dimer of human pancreatic ribonuclease displays specific antitumor activity. *Int. J. Biol. Macromol.* 107, 1965–1970. doi: 10.1016/j.ijbiomac.2017.10.067
- Beintema, J. J. (1998). Introduction: the ribonuclease A superfamily. *Cell Mol Life Sci.* 54, 763–765. doi: 10.1007/s000180050204
- Chang, K. C., Lo, C. W., Fan, T. C., Chang, M. D., Shu, C. W., Chang, C. H., et al. (2010). TNF-alpha mediates eosinophil cationic protein-induced apoptosis in BEAS-2B cells. *BMC Cell Biol.* 11:6. doi: 10.1186/1471-2121-11-6
- Chao, T. Y., and Raines, R. T. (2011). Mechanism of ribonuclease A endocytosis: analogies to cell-penetrating peptides. *Biochemistry* 50, 8374–8382. doi: 10.1021/bi2009079
- Chen, C., Feng, Y., Zou, L., Wang, L., Chen, H. H., Cai, J. Y., et al. (2014). Role of extracellular RNA and TLR3-Trif signaling in myocardial ischemia-reperfusion injury. *J. Am. Heart Assoc.* 3:e000683. doi: 10.1161/JAHA.113.000683
- Chen, J. N., Yang, G. T., Lin, Y. F., Chou, P. L., Wu, T. K., Chang, W. J., et al. (2015). Rana catesbeiana ribonuclease induces cell apoptosis via the caspase-9/-3 signaling pathway in human glioblastoma DBTRG, GBM8901 and GBM8401 cell lines. *Oncol. Lett.* 9, 2471–2476. doi: 10.3892/ol.2015.3117
- Chen, Y., Stevens, B., Chang, J., Milbrandt, J., Barres, B. A., and Hell, J. W. (2008). NS21: re-defined and modified supplement B27 for neuronal cultures. *J. Neurosci. Methods* 171, 239–247. doi: 10.1016/j.jneumeth.2008.03.013
- Cho, S., Beintema, J. J., and Zhang, J. (2005). The ribonuclease A superfamily of mammals and birds: identifying new members and tracing evolutionary histories. *Genomics* 85, 208–220. doi: 10.1016/j.ygeno.2004.10.008
- De Miranda, J., Yaddanapudi, K., Hornig, M., Villar, G., Serge, R., and Lipkin, W. I. (2010). Induction of toll-like receptor 3-mediated immunity during gestation inhibits cortical neurogenesis and causes behavioral disturbances. *MBio* 1, e00176–e00110. doi: 10.1128/mBio.00176-10
- Ferri, R. T., and Levitt, P. (1995). Regulation of regional differences in the differentiation of cerebral cortical neurons by EGF family-matrix interactions. *Development* 121, 1151–1160.
- Folkman, J., and Klagsbrun, M. (1987). Angiogenic factors. *Science* 235, 442–447. doi: 10.1126/science.2432664
- Forrest, C. M., Khalil, O. S., Pizar, M., Smith, R. A., Darlington, L. G., and Stone, T. W. (2012). Prenatal activation of Toll-like receptors-3 by administration of the viral mimetic poly(I:C) changes synaptic proteins, N-methyl-D-aspartate receptors and neurogenesis markers in offspring. *Mol Brain* 5:22. doi: 10.1186/1756-6606-5-22
- Gao, X., and Xu, Z. (2008). Mechanisms of action of angiogenin. *Acta Biochim Biophys Sin.* 40, 619–624. doi: 10.1111/j.1745-7270.2008.00442.x
- Gupta, S. K., Haigh, B. J., Griffin, F. J., and Wheeler, T. T. (2013). The mammalian secreted RNases: mechanisms of action in host defence. *Innate Immun.* 19, 86–97. doi: 10.1177/1753425912446955
- Hung, Y. F., Chen, C. Y., Shih, Y. C., Liu, H. Y., Huang, C. M., and Hsueh, Y. P. (2018). Endosomal TLR3, TLR7, and TLR8 control neuronal morphology through different transcriptional programs. *J. Cell Biol.* 217, 2727–2742. doi: 10.1083/jcb.201712113
- Koczera, P., Martin, L., Marx, G., and Schuerholz, T. (2016). The ribonuclease A superfamily in humans: canonical rnsases as the buttress of innate immunity. *Int. J. Mol. Sci.* 17:E1278. doi: 10.3390/ijms17081278
- Li, S., Sheng, J., Hu, J. K., Yu, W., Kishikawa, H., Hu, M. G., et al. (2013). Ribonuclease 4 protects neuron degeneration by promoting angiogenesis, neurogenesis, and neuronal survival under stress. *Angiogenesis* 16, 387–404. doi: 10.1007/s10456-012-9322-9
- Liu, H. Y., Hong, Y. F., Huang, C. M., Chen, C. Y., Huang, T. N., and Hsueh, Y. P. (2013). TLR7 negatively regulates dendrite outgrowth through the Myd88-c-Fos-IL-6 pathway. *J. Neurosci.* 33, 11479–11493. doi: 10.1523/JNEUROSCI.5566-12.2013
- Lyons, S. M., Fay, M. M., Akiyama, Y., Anderson, P. J., and Ivanov, P. (2017). RNA biology of angiogenin: current state and perspectives. *RNA Biol* 14, 171–178. doi: 10.1080/15476286.2016.1272746
- Mahanthappa, N. K., and Schwarting, G. A. (1993). Peptide growth factor control of olfactory neurogenesis and neuron survival *in vitro*: roles of EGF and TGF-beta s. *Neuron* 10, 293–305. doi: 10.1016/0896-6273(93)90319-M
- Mironova, N., Patutina, O., Brenner, E., Kurilshikov, A., Vlassov, V., and Zenkova, M. (2013). MicroRNA drop in the bloodstream and microRNA boost in the tumour caused by treatment with ribonuclease A leads to an attenuation of tumour malignancy. *PLoS ONE* 8:e83482. doi: 10.1371/journal.pone.0083482
- Mironova, N., Patutina, O., Brenner, E., Kurilshikov, A., Vlassov, V., and Zenkova, M. (2017). The systemic tumor response to RNase A treatment affects the expression of genes involved in maintaining cell malignancy. *Oncotarget* 8, 78796–78810. doi: 10.18632/oncotarget.20228
- Navarro, S., Aleu, J., Jiménez, M., Boix, E., Cuchillo, C. M., and Nogués, M. V. (2008). The cytotoxicity of eosinophil cationic protein/ribonuclease 3 on eukaryotic cell lines takes place through its aggregation on the cell membrane. *Cell Mol. Life Sci.* 65, 324–337. doi: 10.1007/s00018-007-7499-7
- Navarro, S., Boix, E., Cuchillo, C. M., and Nogués, M. V. (2010). Eosinophil-induced neurotoxicity: the role of eosinophil cationic protein/RNase 3. *J. Neuroimmunol.* 227, 60–70. doi: 10.1016/j.jneuroim.2010.06.012
- Okun, E., Griffioen, K. J., Son, T. G., Lee, J. H., Roberts, N. J., Mughal, M. R., et al. (2010). TLR2 activation inhibits embryonic neural progenitor cell proliferation. *J. Neurochem* 114, 462–474. doi: 10.1111/j.1471-4159.2010.06778.x
- Rademacher, F., Simanski, M., and Harder, J. (2016). RNase 7 in cutaneous defense. *Int. J. Mol. Sci.* 17:560. doi: 10.3390/ijms17040560
- Rosenberg, H. F. (2008). RNase A ribonucleases and host defense: an evolving story. *J. Leukoc. Biol.* 83, 1079–1087. doi: 10.1189/jlb.1107725
- Sheng, J., and Xu, Z. (2016). Three decades of research on angiogenin: a review and perspective. *Acta Biochim Biophys. Sin.* 48, 399–410. doi: 10.1093/abbs/gmv131
- Skorupa, A., King, M. A., Aparicio, I. M., Dussmann, H., Coughlan, K., Breen, B., et al. (2012). Motoneurons secrete angiogenin to induce RNA cleavage in astroglia. *J. Neurosci.* 32, 5024–5038. doi: 10.1523/JNEUROSCI.6366-11.2012
- Suzuki, M., Saxena, S. K., Boix, E., Prill, R. J., Vasandani, V. M., Ladner, J. E., et al. (1999). Engineering receptor-mediated cytotoxicity into human ribonucleases by steric blockade of inhibitor interaction. *Nat. Biotechnol.* 17, 265–270. doi: 10.1038/7010
- Tatematsu, M., Nishikawa, F., Seya, T., and Matsumoto, M. (2013). Toll-like receptor 3 recognizes incomplete stem structures in single-stranded viral RNA. *Nat. Commun.* 4:1833. doi: 10.1038/ncomms2857
- Wang, C. L., Tang, F. L., Peng, Y., Shen, C. Y., Mei, L., and Xiong, W. C. (2012). VPS35 regulates developing mouse hippocampal neuronal morphogenesis by promoting retrograde trafficking of BACE1. *Biol Open* 1, 1248–1257. doi: 10.1242/bio.20122451
- Wang, Y. N., Lee, H. H., Chou, C. K., Yang, W. H., Wei, Y., Chen, C. T., et al. (2018). Angiogenin/Ribonuclease 5 is an EGFR ligand and a serum biomarker for erlotinib sensitivity in pancreatic cancer. *Cancer Cell* 33, 752–769.e758. doi: 10.1016/j.ccell.2018.02.012
- Wong, R. W., and Guillaud, L. (2004). The role of epidermal growth factor and its receptors in mammalian CNS. *Cytokine Growth Factor Rev.* 15, 147–156. doi: 10.1016/j.cytogfr.2004.01.004
- Yu, W., Goncalves, K. A., Li, S., Kishikawa, H., Sun, G., Yang, H., et al. (2017). Plexin-B2 mediates physiologic and pathologic functions of angiogenin. *Cell* 171, 849–864.e825. doi: 10.1016/j.cell.2017.10.005
- Zhang, Y., Wang, J., Huang, W., Cai, J., Ba, J., Wang, Y., et al. (2018). Nuclear Nestin deficiency drives tumor senescence via lamin A/C-dependent nuclear deformation. *Nat. Commun.* 9:3613. doi: 10.1038/s41467-018-05808-y

Conflict of Interest Statement: The authors declare that the research was conducted in the absence of any commercial or financial relationships that could be construed as a potential conflict of interest.

Copyright © 2018 Liu, Chen, Hung, Lin, Chao, Shih, Chuang, Li, Huang and Hsueh. This is an open-access article distributed under the terms of the Creative Commons Attribution License (CC BY). The use, distribution or reproduction in other forums is permitted, provided the original author(s) and the copyright owner(s) are credited and that the original publication in this journal is cited, in accordance with accepted academic practice. No use, distribution or reproduction is permitted which does not comply with these terms.